J. KSIAM Vol.16, No.3, 193–204, 2012

NUMERICAL COMPARISON OF WENO TYPE SCHEMES TO THE SIMULATIONS OF THIN FILMS

MYUNGJOO KANG[1], CHANG HO KIM[2], AND YOUNGSOO HA[3*]

[1]DEPARTMENT OF MATHEMATICS, SEOUL NATIONAL UNIVERSITY, SEOUL, SOUTH KOREA
E-mail address: mkang@snu.ac.kr

[2] DEPARTMENT OF COMPUTER ENGINEERING, GLOCAL CAMPUS, KONKUK UNIVERSITY, CHUNGBUK, CHUNGJU,, SOUTH KOREA
E-mail address: kimchang@kku.ac.kr

[3]NATIONAL INSTITUTE FOR MATHEMATICAL SCIENCES, DAEJEON,, SOUTH KOREA
E-mail address: youngsoo@nims.re.kr

ABSTRACT. This paper is comparing numerical schemes for a differential equation with convection and fourth-order diffusion. Our model equation is $h_t + (h^2 - h^3)_x = -(h^3 h_{xxx})_x$, which arises in the context of thin film flow driven the competing effects of an induced surface tension gradient and gravity. These films arise in thin coating flows and are of great technical and scientific interest. Here we focus on the several numerical methods to apply the model equation and the comparison and analysis of the numerical results. The convection terms are treated with well known WENO methods and the diffusion term is treated implicitly. The diffusion and convection schemes are combined using a fractional step-splitting method.

1. INTRODUCTION

In this paper, we consider numerical solutions for the thin film partial differential equations of the form

$$\begin{aligned} &h_t + (h^2 - h^3)_x = -(h^3 h_{xxx})_x, \quad x \in \mathbb{R}, \quad t \geq 0, \\ &h(x,0) = h_0(x), \end{aligned} \tag{1.1}$$

with proper boundary conditions. Equation (1.1) describes the flow of a thin liquid film, where $h(x,t) \geq 0$ denotes the film thickness. The flux terms represent surface shear and gravity, where the forces act in opposing directions and the diffusion term on the right hand side represents surface tension. The surface shear term may arise due to temperature or concentration

Received by the editors April 20 2012 ; Accepted August 13 2012.
2010 *Mathematics Subject Classification.* 93B05.
Key words and phrases. Thin films, WENO schemes, Hyperbolic conservation laws.
The first author's work was supported by Ministry of Culture, Sports and Tourism(MCST) and Korea Creative Content Agency(KOCCA) in the Culture Technology(CT) Research & Development Program.
* Corresponding author.

gradients or to an external shear force (caused by wind for example). A phenomenon of interest in liquid thin film flows under certain conditions is driven by competing effects of the gravity and a thermally induced surface tension gradient. Understanding the thin liquid film is important in many physical systems such as coating processes, de-icing of airplane wings and construction of photographic films. Recently, it has been discovered that the interfacial dynamics of these liquid thin films include the development of undercompressive shocks. Several finite difference schemes have been developed for the simulation of the liquid thin film flows and are available in the literature. The main difference among them is the way they address the problem of shock waves formation.

The model equation is constructed by the fourth order regularization and the nonconvex flux function. Numerical schemes for the solution of nonconvex flux have been successful due to developing high order ENO and Weight ENO schemes. However, it is not proper to treat the fourth order diffusion term with those schemes directly using explicit methods because of too much computing cost. To treat the diffusion terms we have to concern implicit methods.

ENO schemes are using an adaptive stencil from a set of candidate stencils to avoid spurious oscillations near discontinuities. Osher and Shu constructed high order methods based on essentially non-oscillatory (ENO) schemes [7, 6, 15, 17] for solving hyperbolic partial differential equations with several monotone fluxes. In 1994, Liu, Osher, and Chan [11] introduced an weighted ENO (WENO) scheme, which is an improved version of the cell-averaged ENO schemes. WENO uses a nonlinear convex combination of all the candidate stencils by weighting the contribution of the local flux according to its smoothness on each stencil. Jiang and Shu [9] introduced a finite difference (flux) version of WENO schemes (for hyperbolic conservation laws, denoted by WENO-JS) along with new smoothness indicators which are the sum of the normalized squares of the scaled L^2 norms of the all derivatives of the lower order polynomials.

In [8], Henrick, Aslam, and Powers noticed an important limitation of the fifth-order WENO-JS scheme that it may provide only the third-order accuracy at certain smooth extrema or near critical points. To fix this problem, they constructed the so-called Mapped WENO scheme(WENO-M) by using a simple nonlinear mapping to the WENO-JS. Compared to the WENO-JS scheme, the WENO-M scheme can achieve the optimal convergence order at critical points of smooth parts, reduce the numerical dissipation, and obtain sharper results near discontinuities. In [2], Borges, Carmona, Costa, and Don introduced another version of the fifth-order WENO scheme (called WENO-Z) with a new higher order smoothness indicator which is obtained through a linear combination of the smoothness indicator of WENO-JS. The WENO-Z scheme has the same accuracy as the WENO-M scheme but generates improved results.

The goal of this paper is comparing the several numerical solution of the thin film equations. We compare approximate solutions obtained by numerical solutions and discuss effectiveness and accuracy of the numerical schemes.

2. NUMERICAL SCHEMES

In numerical computations, there are several ways to handle convection-diffusion equations which are fractional step splitting methods and unsplit methods. We here consider to solve the equation (1.1) using a fractional step splitting method, in which one alternates between solving the convection equation

$$h_t + f(h)_x = 0 \text{ where } f(h) = h^2 - h^3, \tag{2.1}$$

and the diffusion equation

$$h_t = -(h^3 h_{xxx})_x, \tag{2.2}$$

in each time step. For the diffusion equation we are using Crank-Nicolson methods (see [3]). We now consider a numerical scheme for the convection part,

$$h_t + f(h)_x = 0. \tag{2.3}$$

The notation employed in the numerical calculations is as follows. Let $\{I_j\}$ be a partition of a given domain with the jth cell $I_j := [x_{j-1/2}, x_{j+1/2}]$. The center of I_j is denoted by $x_j = \frac{1}{2}(x_{j-1/2} + x_{j+1/2})$ and the value of a function h at the location x_j is denoted by using the subscript j, i.e., $h_j = h(x_j)$. In what follows, for practical use, we assume that the set $\{x_{j+1/2}\}_j$ is uniformly gridded. Then, the notation $\Delta x = x_{j+1/2} - x_{j-1/2}$ indicates the size of I_j.

The one-dimensional hyperbolic conservation laws in (2.3) can be approximated by a system of ordinary differential equations, where the spatial derivative has been replaced by a finite difference, so that it yields the semi-discrete form:

$$\frac{dh_j}{dt} = -\frac{1}{\Delta x}\big(\hat{f}_{j+1/2} - \hat{f}_{j-1/2}\big), \tag{2.4}$$

where $h_j(t)$ is the numerical approximation to the point value $h(x_j, t)$ in a grid and $\hat{f}_{j+1/2}$ is a numerical flux. The numerical flux $\hat{f}$ has to satisfy a Lipschitz continuity in each of its arguments and is consistent with the physical flux f, that is, $\hat{f}(h, \ldots, h) = f(h)$. To compute the numerical flux $\hat{f}_{j\pm1/2}$, we define a function g implicitly through the following equation (see Lemma 2.1 of [17]),

$$f(h(x)) = \frac{1}{\Delta x}\int_{x-\Delta x/2}^{x+\Delta x/2} g(\xi)d\xi. \tag{2.5}$$

Differentiating (2.5) with respect to x leads to

$$f(h(x))_x = \frac{1}{\Delta x}\Big(g(x + \frac{\Delta x}{2}) - g(x - \frac{\Delta x}{2})\Big), \tag{2.6}$$

which indicates that the numerical flux $\hat{f}_{j\pm1/2}$ should approximate $g(x_{j\pm1/2})$ to a high order, that is, $\hat{f}_{j\pm1/2} = g(x_{j\pm1/2}) + \mathcal{O}(\Delta x^5)$.

2.1. **WENO.** We first briefly introduce the construction of the WENO scheme [9, 18]. In order to construct $\hat{f}_{j+1/2}$, the classical WENO scheme with the fifth-order accuracy uses a 5-point stencil which is subdivided into three candidate substencils. A numerical flux is calculated for each stencil and the local solutions are then averaged in a way of retaining the fifth-order convergence in smooth regions. However, in order to better approximate derivatives near shocks, the weights should effectively remove the contribution of stencils which contain the discontinuity.

To avoid entropy violating solutions and obtain the numerical stability we split the flux $f(h)$ into two components f^+ and f^- such that

$$f(h) = f^+(h) + f^-(h), \tag{2.7}$$

where $\frac{\partial f^+}{\partial h} \geq 0$ and $\frac{\partial f^-}{\partial u} \leq 0$. One of the simplest flux splitting is the Lax-Friedrichs splitting which is given by

$$f^\pm(h) = \frac{1}{2}(f(h) \pm \alpha h), \tag{2.8}$$

where $\alpha = \max_h |f'(h)|$ over the pertinent range of h which can be decided a-priori using the explicit formula for the exact solution.

The interface approximation of the fifth order WENO with Lax-Friedrichs splitting is given by

$$\begin{aligned} f(h^n_{j+1/2}) = \; & \tfrac{1}{12}(-f_{j-1} + 7f_j + 7f_{j+1} - f_{j+2}) - \Phi_N(\Delta f^+_{j-\frac{3}{2}}, \Delta f^+_{j-\frac{1}{2}}, \Delta f^+_{j+\frac{1}{2}}, \Delta f^+_{j+\frac{3}{2}}) \\ & + \Phi_N(\Delta f^-_{j+\frac{5}{2}}, \Delta f^-_{j+\frac{3}{2}}, \Delta f^-_{j+\frac{1}{2}}, \Delta f^-_{j-\frac{1}{2}}), \end{aligned} \tag{2.9}$$

where $f_j = f(h^n_j)$, $f^\pm_j = f^\pm(h^n_j)$, $\Delta f^\pm_{i+\frac{1}{2}} = f^\pm_{i+1} - f^\pm_i$ and

$$\Phi_N(a, b, c, d) = \frac{1}{3}\omega_0(a - 2b + c) + \frac{1}{6}(\omega_2 - \frac{1}{2})(b - 2c + d). \tag{2.10}$$

2.2. **WENO-JS.** The smoothness indicator β_j developed by Jiang and Shu [9] is given by

$$\beta_k = \sum_{\ell=1}^{2} \int_{x_{j-1/2}}^{x_{j+1/2}} \Delta x^{2\ell-1} \Big(\frac{d^\ell}{dx^\ell} \hat{f}^k \Big)^2 dx. \tag{2.11}$$

The weights ω_i and d_i are defined by

$$\omega_j = \frac{\alpha_j}{\sum_{l=0}^{2} \alpha_l} \, , \; \alpha_l = \frac{d_l}{(\varepsilon + \beta_l)^2} \, , \tag{2.12}$$

$$d_0 = \frac{1}{10} \, , \; d_1 = \frac{3}{5} \, , \; d_2 = \frac{3}{10} \, , \tag{2.13}$$

where $0 < \varepsilon$ is taken to prevent singularity.

We remark that the indicator in (2.11) is similar to, but smoother than, the total variation measurement based on the L^1 norm. For more details, the readers are referred to [18].

2.3. **Mapped WENO.** Henrick, Aslam, and Powers [8] noticed that the convergence order may not hold at certain smooth extrema or near critical points in WENO-JS. To fix this problem, they introduced a mapping function $g_k(\omega)$ defined as

$$g_k(\omega) = \frac{\omega(d_k + d_k^2 - 3d_k\omega + \omega^2)}{d_k^2 + \omega(1 - 2d_k)}, \quad k = 0, 1, 2, \tag{2.14}$$

where d_k are the ideal weights given in (2.12) and $\omega \in [0, 1]$. This function is a non-decreasing monotone function in [0, 1] with the following properties:
1. $0 \leq g_k(\omega) \leq 1$, $g_k(0) = 0$ and $g_k(1) = 1$.
2. $g_k(\omega) \approx 0$ if $\omega \approx 0$; $g_k(\omega) \approx 1$ if $\omega \approx 1$.
3. $g_k(d_k) = d_k$, $g_k'(d_k) = g_k''(d_k) = 0$.
4. $g_k(\omega) = d_k + \mathcal{O}(\Delta x^6)$, if $\omega = d_k + \mathcal{O}(\Delta x^2)$.
The mapped weights are given by:

$$\omega_k^M = \frac{\alpha_k^M}{\sum_{\ell=0}^2 \alpha_\ell^M}, \quad \alpha_k^M = g_k(\omega_k), \quad k = 0, 1, 2, \tag{2.15}$$

where ω_k are computed via (2.12).

2.4. **WENO-Z.** The idea of the fifth order WENO-Z scheme introduced in [2] is the modification of the smoothness indicator β_k of WENO-JS to obtain a higher order smoothness indicator. This new smoothness indicator of the fifth order WENO-Z is obtained by the linear combination of the β_k to satisfy the sufficient condition for fifth order convergence.

The nonlinear weights ω_k^z of WENO-Z are defined by

$$\omega_k^z = \frac{\alpha_k^z}{\sum_{\ell=0}^2 \alpha_\ell^z} \quad \text{and} \quad \alpha_k^z = \frac{d_k}{\beta_k^z} \tag{2.16}$$

where d_k are the ideal weights given in (2.13) and the new smoothness indicator β_k^z are defined by

$$\beta_k^z = \left(1 + \left(\frac{|\beta_0 - \beta_2|}{\beta_k + \varepsilon}\right)^2\right).$$

If we have a numerical approximation to each of the spatial terms we can rewrite this equation for the fixed time t as an ordinary differential equation (ODE)

$$\frac{dh(t)}{dt} = \mathcal{L}(h^n),$$

where $\mathcal{L}(h^n)$ is a discretization of the spatial operator. To retain high-order accuracy in time without creating spurious oscillations, it is customary to use so-called TVD Runge-Kutta methods [15, 17] as the ODE solver. These methods employ a convex combination of forward Euler steps to advance the solution in time. They are especially designed to maintain the TVD

property, i.e., ensure that the solution is total variation diminishing, the third-order method (RK-TVD3) reads:

$$\begin{aligned} h^{(1)} &= h^n + \Delta t \mathcal{L}(h^n) \\ h^{(2)} &= \frac{3}{4}h^n + \frac{1}{4}h^{(1)} + \frac{1}{4}\Delta t \mathcal{L}(h^{(1)}) \\ h^{n+1} &= \frac{1}{3}h^n + \frac{2}{3}h^{(2)} + \frac{2}{3}\Delta t \mathcal{L}(h^{(2)}), \end{aligned}$$

where h^n represents the solution at the time step n.

3. Numerical Results

In this section we present the numerical results using WENO-JS, WENO-M and WENO-Z methods.

Example 3.1. Let us consider the equation of the non-convex flux

$$\begin{aligned} & q_t + (q^2 - q^3)_x = 0, \\ & q(x,0) = \begin{cases} 2/3, & \text{if } 0 \le x \le 1, \\ 0, & \text{otherwise.} \end{cases} \end{aligned} \tag{3.1}$$

Since the flux function is non-convex, the exact solution has slightly more structures than that of a convex flux function. The solution can be computed by using rarefaction waves and the equal area rule. The solution is integrated up to $t = 20$ with $\Delta x = 0.01$ in the calculations. The CFL number is set to 0.5. The results are shown in Figs. 1. The WENO-Z methods are overestimated but Mapped WENO performs better than the classical WENO schemes.

Now we consider the original problem (Eqs. (1.1)) and compare the results of WENO-JS, WENO-M and WENO-Z methods. To solve the equation numerically, we employ a fractional step splitting method that alternates between solving the diffusion equation (2.2) and the convection equation (2.1). In the following examples, when we employ an explicit scheme to the convection term, we calculate the diffusion term using the Crank-Nicolson scheme. To clearly distinguish between the different schemes and to avoid differences caused by the behavior due to the initial condition, it is best to compare results at large times. And this needs to large computational domains and consequently large computation times. In most examples we therefore modify equation (1.1) to move with the region of interest

$$h_t + (h^2 - h^3)_x - s h_x = -(h^3 h_{xxx})_x \tag{3.2}$$

where the wave speed s is the shock speed given by the Rankine-Hugoniot condition using the two boundary values

$$s = \frac{f(h_r) - f(h_r)}{h_r - h_r}. \tag{3.3}$$

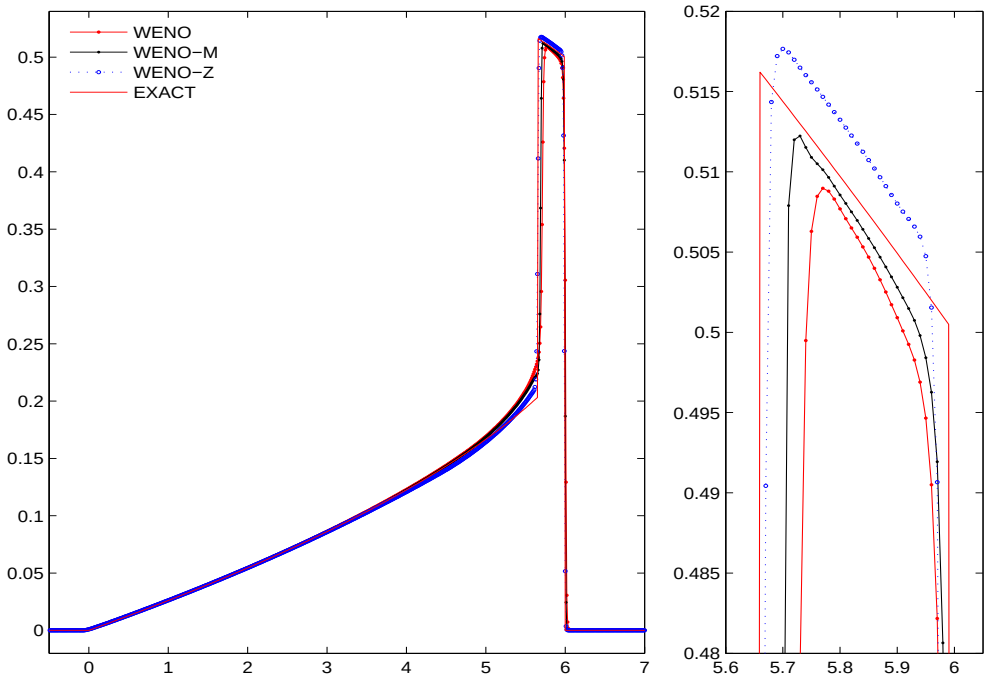

FIGURE 1. Comparison of the analytical solution with the numerical solution of non-convex flux function (3.1) with WENO-JS, WENO-M and WENO-Z at $t = 20$.

We now consider the results of the numerical schemes of adding the term $-sh_x$ to the traveling wave. For consistency and to prevent the numerical treatment of the $-sh_x$ term from affecting the results, we apply the central method to this term for all schemes. This indicates a good reason to use the explicit schemes, which show consistent results regardless of the initial data. In the numerical results of the thin film equation, the change of initial conditions can observe the various behavior of propagating waves.

Now, we consider the multiple Lax shock profiles and compare the results of several initial conditions. First we consider the following condition:

Example 3.2.

$$h(x) = (\tanh(-x + 300) + 1)\frac{h_\infty - b}{2} + b \tag{3.4}$$

where $h_\infty = 0.3323$ and $b = 0.1$. The results are shown in fig. 2.

The second stable wave involves an initial condition with a bump of width 10,

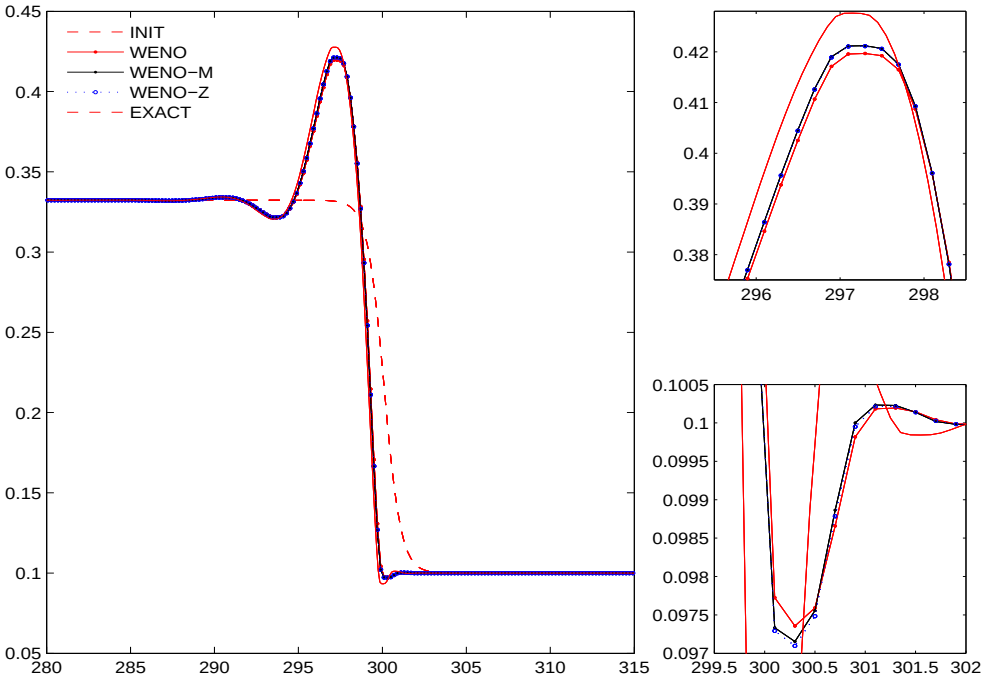

FIGURE 2. Comparison of the analytical solution with the numerical solution of non-convex flux function (3.1) with WENO-JS, WENO-M and WENO-Z at $t = 10^4$.

Example 3.3.

$$h(x) = \begin{cases} ((0.6 - h_\infty)/2)\tanh(x - 300) + (0.6 + h_\infty)/2, & \text{if } x < 305, \\ -((0.6 - b)/2)\tanh(x - 310) + (0.6 + b)/2, & \text{otherwise.} \end{cases} \tag{3.5}$$

In Fig. 3 we present results for the initial profile of Eq. (3.5) at $t = 10^4$. In this case we solve the governing equation with a moving axis, given by Eq. (3.2). The CFL numbers for the schemes are 0.5. The results of Mapped WENO and WENO-Z methods are hard to distinguish. All curves show that the initial hump changes to an undercompressive wave on the right and a compressive wave on the left. The bump width remains relatively constant for each scheme. This wave therefore appears stable.

The last stable wave involves an initial condition with a bump of width 20 switched the initial condition,

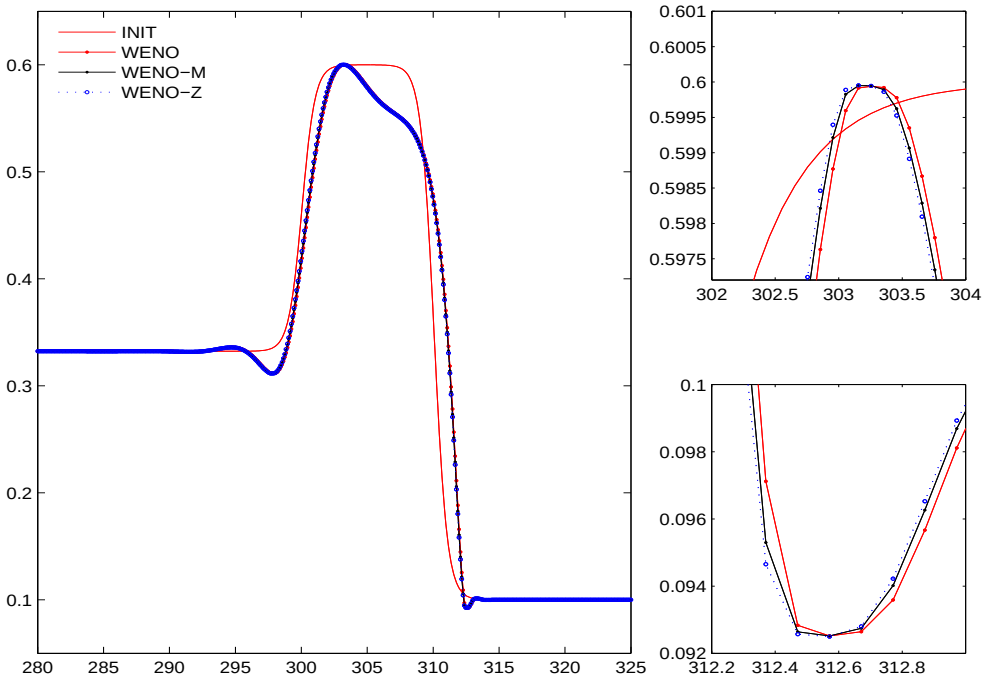

FIGURE 3. Comparison of with WENO-JS, Mapped WENO5 and WENO-Z at $t = 10^4$.

Example 3.4.

$$h(x) = \begin{cases} ((0.6 - h_\infty)/2)\tanh(x - 300) + (0.6 + h_\infty)/2, & \text{if } x < 310, \\ -((0.6 - b)/2)\tanh(x - 320) + (0.6 + b)/2, & \text{otherwise.} \end{cases} \tag{3.6}$$

The results are shown in Fig. 4 at $t = 10^5$. We set the CFL numbers equal 0.5. Ha et. al. [3] point out that the WENO-JS methods are relatively stable than the other explicit methods. We can see that the other WENO schemes - WENO-Z and WENO-M - are stable.

4. CONCLUSION

We have presented the results of a fourth-order thin film equations using several numerical schemes. We apply fractional step-splitting method using an explicit scheme for the convection term and an implicit one for the fourth-order diffusion term. When the fourth-order diffusion term is included, it is clear that implicit methods should be applied to speed up calculations. For each method, our choice led to the best results in the example of Section 3. WENO-M provided consistent and accurate results. When the convective term $-sh_x$ was included, the

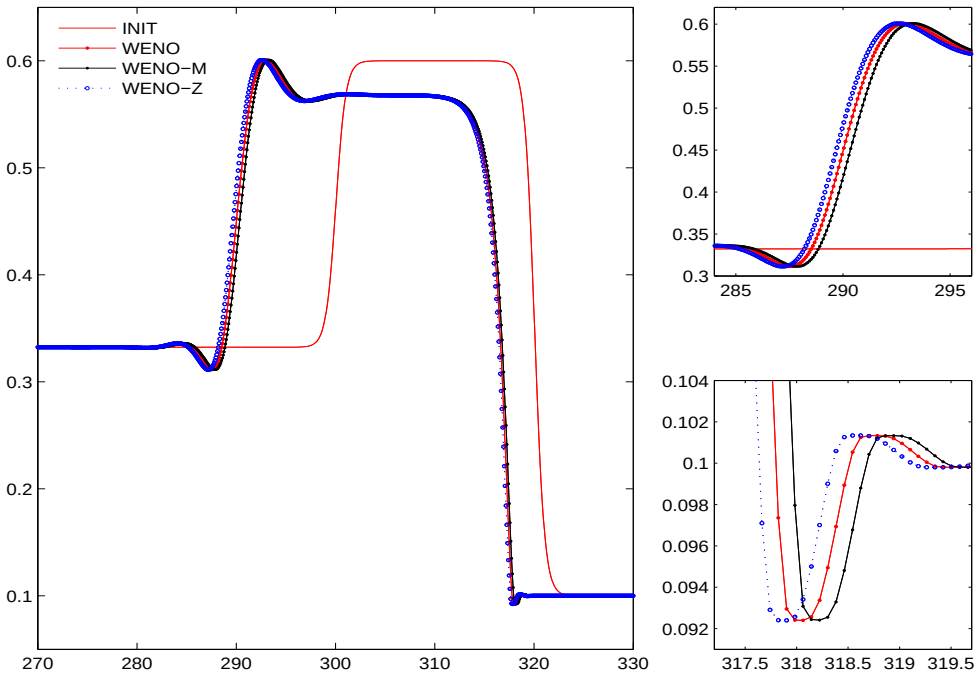

FIGURE 4. Comparison of WENO-JS, WENO-M and WENO-Z at $t = 10^5$.

problem with the implicit schemes was removed. This was a result of applying the central method to this term which gave the scheme a similar form to our other explicit schemes.

To summarize, from our calculations, it appears that for the best accuracy and efficiency fourth-order diffusion equations with a convective term should be tackled using an explicit method on the convection term coupled to an implicit diffusion term by fractional step-splitting. The choice of explicit methods may be guided by a traveling wave solution. Our examples indicate that, for this type of problem, WENO-M is the most robust of the three methods investigated.

Acknowledgements Myungjoo Kang was supported by the National Research Foundation of Korea(NRF) funded by the Ministry of Education, Science and Technology(2012001766) and by Ministry of Culture, Sports and Tourism(MCST) and Korea Creative Content Agency(KOCCA) in the Culture Technology(CT) Research & Development Program(R2011050089).

REFERENCES

[1] A.L. Bertozzi, A. Munch, M. Shearer, Undercompressive shocks in thin film flows, *Physica D* **134** 431-464 (1999).

[2] R. Borges, M. Carmona, B. Costa, and W.S. Don, An improved WENO scheme for hyperbolic conservation laws, *J. Comput. Phys.* 227, 3191–3211 (2008).

[3] Y. HA, Y.-J. KIM, AND T.G. MYERS, On the numerical solution of a driven thin film equation, *J. Comput. Phys.* **227**, 7246-7263 (2008).

[4] Y. Ha, C.L. Gardner, A. Gelb, and C.W. Shu Numerical Simulation of High Mach Number Astrophysical Jets with Radiative Cooling *JSC* **24**, 29-44 (2005).

[5] A. Harten, P.D. Lax, B. van Leer, On upstream differencing and Godunov-type schemes for hyperbolic conservation laws, *SIAM Rev.* **25**, 35 (1983).

[6] A. Harten, On a Class of High Resolution Total-Variation-Stable Finite-Difference Schemes, *SIAM J. Numer. Anal.*,Vol. 21, no. 1, 1-23 (1984).

[7] A. Harten and G. Zwas, Self-Adjusting Hybrid Schemes for Shock Computations, *J. Comput. Phys.* **9**, 568-583 (1973).

[8] A.K. Henrick, T.D. Aslam, and J.M. Powers, Mapped weighted-essentially-non-oscillatory schemes : achieving optimal order near critical points, *J. Comput. Phys.* 207, 542–567 (2005).

[9] G-S. Jiang and C.-W. Shu, Efficient implementation of weighted ENO schemes, *J. Comput. Phys.*, 126 (1996), pp. 202–228.

[10] P. D. Lax and B. Wendroff, Systems of conservation laws, *Communications in Pure and Applied Mathematics* **13**, 217(1960).

[11] X-D. Liu, S. Osher, and T. Chan, Weighted essentially non-oscillatory schemes, *J. Comput. Phys.*, 115 (1994), pp. 200–212.

[12] R. J. LeVeque, Numerical Methods for Conservation Laws, *Birkhauser Verlag*, Basel (1992).

[13] P. L. Roe, Approximate Riemann solvers, paremeter vectors, and difference schemes, *J.Comp. Phys.*,**43**, 357-372(1981).

[14] T. Schmutzler and W. M. Tscharnuter, Effective radiative cooling in optically thin plasmas, *Astronomy and Astrophysics* **273**, 318-330, (1993).

[15] C.-W. Shu, Total-variation-diminshing time discretizations *SIAM J. Sci. Statist. Comput.* **9**, 1073-1084 (1988).

[16] C.-W. Shu and S. Osher, Efficient implementation of essentially non-oscillatory shock capturing schemes, *J. Comput. Phys.* **77**, 32 (1988).

[17] C.-W. Shu and S. Osher, Efficient implementation of essentially non-oscillatory shock capturing schemes,II, *J. Comput. Phys.* **83**, 32-78 (1989).

[18] C.W. Shu, ENO and WENO schemes for hyperbolic conservation laws, in: B. Cockburn, C. Johnson, C.W. Shu, E. Tadmor (Eds.), Advanced Numerical Approximation of Nonlinear Hyperbolic Equations, Lecture Notes in Mathematics, vol. 1697, Springer, Berlin, 1998, pp. 325–432 (also NASA CR- 97-206253 and ICASE-97-65 Rep., NASA Langley Research Center, Hampton [VA, USA]).

[19] P. K. Sweby, High resolution schemes using flux limiters hyperbolic conservation laws, *SIAM J.Numer. Anal.* **Vol. 21**, No.5, 995-1011(1984).

[20] E. F. Toro, Riemann Solvers and Numerical Methods for Fluid Dynamics, *Springer-Verlag* , New York (1997).

[21] R.J. LEVEQUE, *Numerical methods for conservation laws*, Lectures in Mathematics ETH Zürich, Birkhäuser Verlag, Basel, 1990.

[22] R.J. LEVEQUE, High-resolution conservative algorithms for advection in incompressible flow. *SIAM J. Sci. Compu.* , 1995.

[23] R.J. LEVEQUE, *Clawpack Version 4.0 Users Guide*, Technical report, University of Washington, Seattle, 1999. Available online at http://www.amath.washington.edu/∼claw/.

[24] H. NESSYAHU AND E. TADMOR, *Nonoscillatory central differencing for hyperbolic conservation laws*, J. Comput. Phys., 87 (1990), no. 2, 408–463.

[25] B. VAN LEER, *MUSCL, A New Approach to Numerical Gas Dynamics.* In Computing in Plasma Physics and Astrophysics, Max-Planck-Institut fűr Plasma Physik, Garchung, Germany, April 1976.
[26] A.L. BERTOZZI, A. MUNCH, M. SHEARER, *Undercompressive shocks in thin film flows* Physica D 134 (1999) 431-464